Hindawi Publishing Corporation
International Journal of Tissue Engineering
Volume 2013, Article ID 407047, 9 pages
http://dx.doi.org/10.1155/2013/407047

Research Article

Biomanufacturing versus Superficial Cell Seeding: Simulation of Chondrocyte Proliferation in a Cylindrical Cartilage Scaffold

Mohammad Izadifar

Division of Biomedical Engineering, College of Engineering, University of Saskatchewan, Saskatoon, SK, Canada S7N 5A9

Correspondence should be addressed to Mohammad Izadifar; moi333@mail.usask.ca

Received 23 March 2013; Revised 18 May 2013; Accepted 20 May 2013

Academic Editor: Eng San Thian

Local volume averaging approach was used for modeling and simulation of cell growth and proliferation, as well as glucose transfer within a cylindrical cartilage scaffold during cell cultivation. The scaffold matrix including the nutrient solution filling spaces among seeded cell colonies was treated as a porous medium. Applying differential mass balance of cells and glucose to a representative elementary volume of the scaffold, two diffusional mass transfer models were developed based on local volume averaged properties. The derived governing equations take into account time-dependent glucose diffusion, glucose consumption by cells, cell migration, apoptosis, and cell reproduction within the scaffold. Since the volumetric fraction of cells in the scaffold relies on cell growth, which strongly depends on glucose concentration in the scaffold, the governing equations were solved simultaneously using implicit finite difference method and Gauss-Seidel technique. Simulation results showed that cell volumetric fraction of the scaffold can reach about 45% after 50 days if a culture medium with a glucose concentration of 45 kgm^{-3} is used. Also, simulation results indicate that more uniform and higher average cell volume fraction of the scaffold can be obtained if biomanufacturing-based cell seeding is used across the scaffold rather than cell seeding on the scaffold surface.

1. Introduction

Nowadays tissue engineering has extensively attracted the attention of researchers to the development of biological substitutes for repairing or maintaining damaged tissues. Principally three therapeutic strategies which can be adopted for treating a damaged tissue are (i) implantation of precultivated cells; (ii) implantation of preassembled tissues which have been regenerated *in vitro*; (iii) implantation of biocompatible and biodegradable scaffolds containing live cells for *in situ* regeneration. In the third strategy, live cells and growth factors are incorporated in a degradable scaffold which is implanted in the damaged tissue where growth of both tissue cells and cells in the scaffold promotes tissue healing [1]. A cell-scaffold can be made of natural materials such as chitosan, collagen, and glycosaminoglycans or synthetic materials such as polyglycolic acid (PGA), polylactic acid (PLA), and polycaprolactone (PCL) by means of a biomanufacturing fabrication method.

The scaffold features must satisfy some crucial conditions. The porosity of the scaffold should be sufficiently high to facilitate cell growth, cell migration, and nutrient transfer as well as transport of metabolic waste. Also, the scaffold must be biocompatible in order to prevent the scaffold to be rejected by the body after implantation. In addition, while the scaffold should be sufficiently compliant not to damage surrounding tissues, it must be strong enough to support load forces and not to structurally collapse in the implanted site until the hard tissue transplant has been remodeled [2].

Cartilage/bone tissue engineering has been extensively investigated by researchers and has been found a promising technique in biomedical engineering [2]. The tissue cells including osteoblasts and chondrocytes are taken from the patient's hard and soft tissues followed by cell manipulation and expansion in a culture [3]. Expanded cells are seeded onto a biodegradable scaffold in a culture (i.e., petri dish or bioreactor) to allow cells to proliferate in the scaffold. When cells are sufficiently expanded in the scaffold, the cell-scaffold is transplanted by surgery. It is required for the biodegradable scaffold to retain its physical properties (i.e., stiffness) for at least 6 months including 4 months for cell culturing and 2 months *in situ* [4].

In vitro cell proliferation on the scaffold is a crucial step which must be conducted in a well-controlled environment for a successful and efficient *in vitro* engineering of the scaffold construct for clinical use. For a scaffold fabricated by a biomanufacturing technique, cells have been already incorporated in the scaffold. Growth and proliferation of cells strongly rely on the scaffold porosity and nutrient diffusion from the culture environment into the scaffold.

One of the challenges in cartilage tissue engineering is to fabricate cell-scaffold constructs possessing clinically proper dimensions and filled with neo cells [5]. This challenge is associated with the diffusion limits of the nutrients (i.e., glucose) throughout the cell-scaffold which can delay cell growth and proliferation in the scaffold. This difficulty may be resolved by developing highly porous scaffolds to facilitate the transportation of nutrients and metabolite wastes in the scaffold. Also, properly designed hydrodynamic bioreactors can be used for enhancing transportation of nutrients into the scaffold [6]. For developing a cell-scaffold, mathematical modeling and simulation of nutrient transfer and cell growth during cell cultivation seem crucial for analyzing the sensitivity of cell proliferation with respect to *in vitro* culture conditions (i.e., glucose concentration of the culture in the petri dish or bioreactor) as well as scaffold structural properties (i.e., dimension, geometry, and initial porosity).

An empirical equation was developed by Freed et al. [7] to investigate the cell culture in a PGA scaffold. Lewis et al. [8] developed a model for analysis of cell density distribution and oxygen concentration. Galban and Locke [9] developed a mechanistic model based on volume average method to describe the distribution of glucose concentration and cell density in a cell-construct structure. Mathematical models have confirmed the diffusion limit over cell growth in a cell-scaffold. Chung et al. [5] developed mathematical model incorporating cell mobility due to random walk to describe the interaction between cell proliferation and nutrient transfer using COMSOL for a cell-scaffold with slab geometry.

Generally, there are some stages towards the implantation of an engineered tissue. These stages can be briefly summarized as (i) cell sourcing from the patient, (ii) cell culture and expansion *in vitro*, (iii) cell seeding on a scaffold or incorporating the cells into the scaffold using biomanufacturing fabrication method, (iv) cell growth and cell proliferation in the scaffold by subjecting the cell-scaffold to a static or dynamic culture medium, and (v) transplantation of the cell-scaffold [5]. This study focuses on stage iv, cell cultivation on the scaffold in static media (petri dish). The main objective of this study is mathematical modeling and simulation of cell growth, cell migration, and nutrient transfer in a cylindrical cartilage cell-scaffold using local volume averaging approach during *in vitro* cell proliferation. Also, a sensitivity analysis of cell proliferation is performed with respect to scaffold dimension and glucose concentration of *in vitro* culture environment.

2. Theory

In tissue engineering, cell culture and proliferation is an important stage during which the volumetric fraction of cells in the scaffold sufficiently increases so that the scaffold becomes ready for transplantation. The time for cell proliferation on the scaffold depends on the scaffold dimension, porosity, and initial population and distribution of seeded cells. The scaffold geometry should match the implant site of the injured tissue. The porosity of the scaffold should be sufficiently high to enhance the transportation of nutrients into the scaffold. The initial population as well as distribution of cells in the scaffold relies on the type of cell seeding. Biomanufacturing fabrication methods can provide scaffolds with more uniform cell distribution in the scaffold than the method of cell seeding on the scaffold surface. The effect of these factors on the cell growth and cell volumetric fraction during cell culture can be simulated and analyzed for a cylindrical cell-scaffold which can be potentially used for neural or cartilage/bone tissue engineering. Since important properties including cell metabolite and growth kinetics, which are required for modeling and simulation, have been already reported for cartilage cells, the mathematical modeling and simulation are applied to a cartilage cell-scaffold; however, the model can be used for other applications by applying the related properties to the model.

2.1. Local Volume Averaging (LVA) and Local Equilibrium. The cell-scaffold is in fact a porous medium which is a solid matrix consisting of a solid phase, cell colonies and scaffold structure, and spaces among solid particles which are filled with a fluid, nutrient solution. The range of pore size of porous media can vary from molecular size (nm) to centimetre. When a solid matrix cannot be described within pore size, a representative elementary volume (REV) with a characteristic length (l) and volume (V_l) is defined to represent the structure of the solid matrix. REV is defined as the smallest differential volume of a porous medium that results in statistically meaningful average properties of the porous medium [12]. Figure 1 illustrates a schematic diagram of a cylindrical scaffold with a radius and height of ≈1.5 and 3 mm, respectively. The pore size of the cell-scaffold can be represented by the length scales of a cell colony and the nutrient phase in an REV which are ≈11 and 14 μm, respectively [9].

Averaging properties of the medium over the REV are called local volume average properties, and averaging properties of a phase over the volume of the phase in the REV are called intrinsic average properties. Local and intrinsic average properties are defined as.

$$\langle \vartheta \rangle = \frac{1}{V_{\mathrm{REV}}} \int_{V_{\mathrm{REV}}} \vartheta \, dV. \tag{1}$$

In the same way,

$$\left\langle \xi_p \right\rangle^p = \frac{1}{V_p} \int_{V_p} \xi_p dV, \tag{2}$$

where V_{REV}, V_p, $\langle \vartheta \rangle$, and $\langle \xi_p \rangle^p$ are REV, the phase volume, local volume average, and intrinsic average properties, respectively.

For the cell-scaffold, as shown in Figure 1, local and intrinsic average properties are volumetric cell fraction, ε_c,

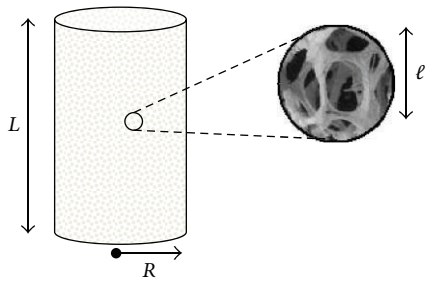

Figure 1: Schematic diagram of a cylindrical cell-scaffold and REV of the scaffold.

volumetric nutrient fraction, ε_f, intrinsic glucose concentrations in cell colony phase, $\langle C_c \rangle^c$, and in the fluid phase, $\langle C_f \rangle^f$, and average cell density in the phase of cell colony, $\langle \rho_c \rangle^c$. The validity of LVA approach can be assessed by a length scale inequality condition as

$$d_p < l \ll R, L, \tag{3}$$

where d_p is the pore size (length scale of cell colony and nutrient phase), l is REV characteristic length, and R and L are the radius and height of the cell-scaffold construct. Since REV characteristic length of 50×10^{-6} m is larger than the pore sizes of 11×10^{-6} m (size of cell colony) and 14×10^{-6} m (length scale of the fluid phase) and also much smaller than the radius (1.5×10^{-3} m) and height (3×10^{-3} m) of the cell-scaffold construct, the length scale inequality condition is satisfied and LVA is valid for the cell-scaffold system.

If the mass transfer resistance of the solid phase is small enough (low mass transfer Biot number), it can be assumed that the solid phase, the cell colony, is locally in equilibrium with the fluid phase, culture medium. The local equilibrium condition can be expressed as

$$\langle C_c \rangle^c = \lambda \langle C_f \rangle^f, \tag{4}$$

where λ is the partition coefficient relating a nutrient component concentration in the cell colony phase to that in the fluid phase at the equilibrium condition.

2.2. Mathematical Modeling. Glucose which is among the most important nutrients for human cells is considered as the nutrient component for developing a mathematical model. After the cell-scaffold construct is placed in a static culture (i.e., petri dish) containing glucose, cell colonies start absorbing glucose from the fluid phase filling spaces among cell colonies. Glucose consumption by cells reduces glucose concentration of the fluid phase and results in a glucose concentration gradient across the scaffold. Therefore, glucose diffuses from the surrounding culture medium to the inside of the scaffold. At the same time, cell proliferation takes place in the scaffold due to cell growth and cell migration [13]. Cell migration can be analogous to molecular diffusion where cells can migrate from a place with higher cell population to another place with lower cell population due to cell random walks. Cell colony proliferation depends on the nutrient concentration available to cells. Therefore, any glucose concentration in the cell-scaffold construct affects cell growth in the scaffold.

Figure 2 illustrates the schematic diagram of an element of the cell-scaffold where glucose transport takes place along the height and radius of the scaffold due to molecular diffusion, and it is consumed by cell colonies in the scaffold. Also, cell migration can be analogously described by a diffusion model where the cell mobility in the medium can be represented by a cell diffusion coefficient, D_{cell}. In addition to cell migration, cell generation and apoptosis (regulated cell death) should be incorporated in the modeling.

As it is shown in Figure 2, glucose diffuses into the porous cell-scaffold through the network of cell colonies as well as the fluid phase. Applying local equilibrium condition, (4), and diffusional mass transfer to the solid and fluid phases of the element (Figure 2), mass conservation of glucose over the element leads to a two-dimensional partial differential equation as

$$\begin{aligned} &\frac{\partial \left(\left(\lambda \varepsilon_c + \varepsilon_f \right) \left\langle C_f \right\rangle^f \right)}{\partial t} \\ &\quad = \frac{1}{r} \frac{\partial \left(\left(D^c_{\text{eff}} r \varepsilon_c \lambda + D^f_{\text{eff}} r \varepsilon_f \right) \left(\partial \left\langle C_f \right\rangle^f / \partial r \right) \right)}{\partial r} \\ &\qquad + \frac{\partial \left(\left(D^c_{\text{eff}} \varepsilon_c \lambda + D^f_{\text{eff}} \varepsilon_f \right) \left(\partial \left\langle C_f \right\rangle^f / \partial z \right) \right)}{\partial z} \\ &\qquad - K \lambda \varepsilon_c \left\langle C_f \right\rangle^f. \end{aligned} \tag{5}$$

Assuming intrinsic average cell density, $\langle \rho_c \rangle^c$, is constant with time and with position, applying (4) and mass conservation of cells to the element of the cell-scaffold (Figure 2) results in

$$\begin{aligned} \frac{\partial \varepsilon_c}{\partial t} &= \frac{1}{r} \frac{\partial \left(D_{\text{cell}} r \left(\partial \varepsilon_c / \partial r \right) \right)}{\partial r} + \frac{\partial \left(D_{\text{cell}} \left(\partial \varepsilon_c / \partial z \right) \right)}{\partial z} \\ &\quad + k_g \varepsilon_c \left[\frac{\lambda \left\langle C_f \right\rangle^f}{k_c \rho_{\text{cell}} \varepsilon_c + \lambda \left\langle C_f \right\rangle^f} \right] - k_a \varepsilon_c. \end{aligned} \tag{6}$$

For simplifying the resulted partial differential equations, some assumptions were made as follows.

(i) As the scaffold is placed standwise in the petri dish, the scaffold bottom is completely in contact with the petri dish bottom, and it is assumed that no mass transfer takes place from the bottom side of the scaffold to the scaffold construct.

(ii) There is no bulk flow of the nutrients through the scaffold during the cell culture, and therefore the hydrodynamic shear stress within the scaffold can be neglected.

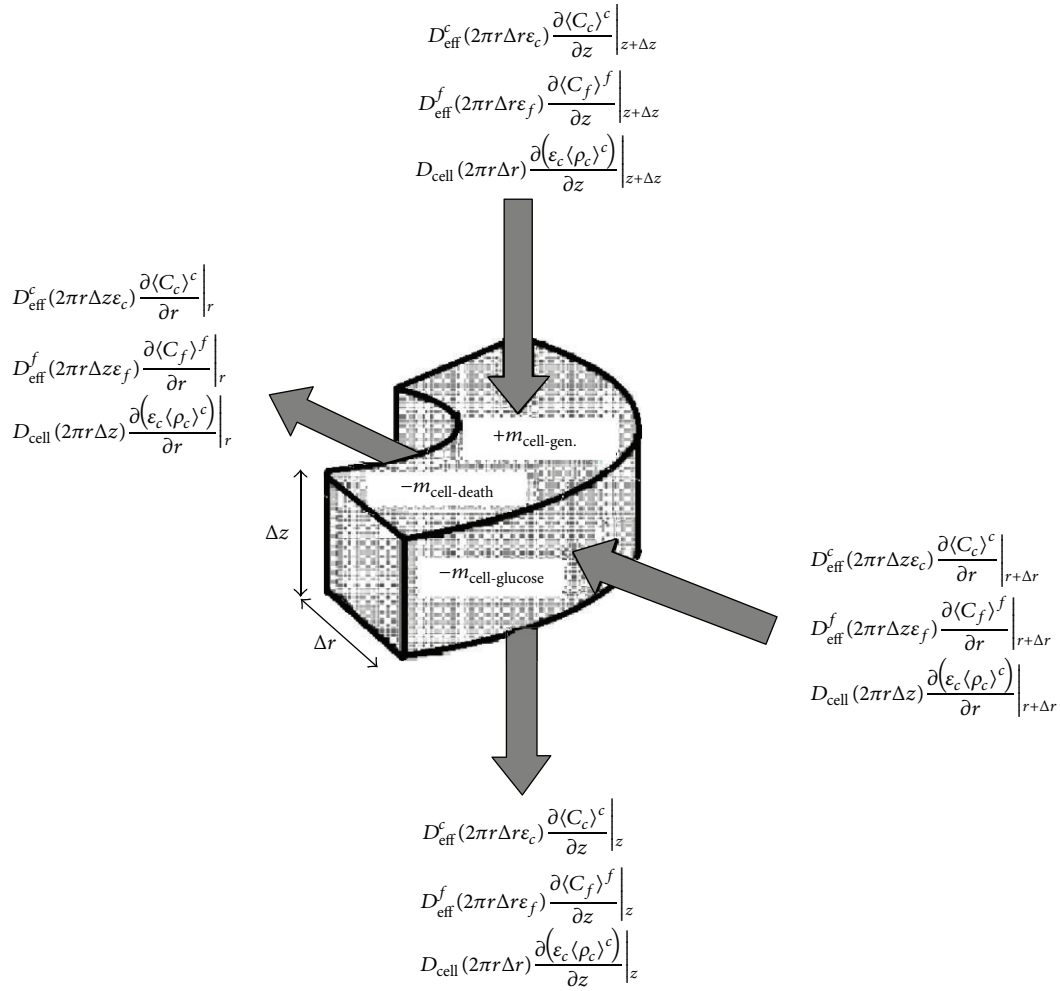

Figure 2: Schematic diagram for mass conservation of glucose over an element of the cell-scaffold construct.

(iii) Only radial mass transfer and cell proliferation take place in the scaffold.

(iv) Glucose concentration of the surrounding culture medium is fixed and equal to the glucose concentration of the fluid phase at the surface of the scaffold.

(v) No cell migration takes place from the scaffold surface to the surrounding culture medium.

(vi) Biomanufacturing-based cell seeding method can provide an initially uniform cell distribution within the scaffold.

(vii) The scaffold is assumed to be an isotropic porous medium resulting in isotropic tensors of diffusion coefficients.

(viii) Cell diffusion coefficient is constant and isotropic.

Applying the assumption of negligible mass transfer in z direction and rearranging (5) and (6), the governing equations of radial glucose transfer and cell proliferation in the cell-scaffold can be expressed as

$$\begin{aligned}\frac{\partial\left\langle C_f\right\rangle^f}{\partial t} &= \left[\frac{(1-\lambda)\left\langle C_f\right\rangle^f}{\delta}\right]\frac{\partial\varepsilon_c}{\partial t} \\ &+ \left[\frac{\alpha}{\delta}+\frac{\beta}{\delta}\left(\frac{\partial\varepsilon_c}{\partial r}\right)\right]\frac{\partial\left\langle C_f\right\rangle^f}{\partial r} \\ &+ \left(\frac{\beta\varepsilon_c+\varepsilon\ D^f_{\text{eff}}}{\delta}\right)\frac{\partial^2\left\langle C_f\right\rangle^f}{\partial r^2} \\ &- \left(\frac{K\lambda\varepsilon_c\left\langle C_f\right\rangle^f}{\delta}\right),\end{aligned} \tag{7}$$

$$\begin{aligned}\frac{\partial\varepsilon_c}{\partial t} &= D_{\text{cell}}\left(\frac{1}{r}\frac{\partial\varepsilon_c}{\partial r}+\frac{\partial^2\varepsilon_c}{\partial r^2}\right) \\ &+ k_g\varepsilon_c\left(\frac{\lambda\left\langle C_f\right\rangle^f}{k_c\rho_{\text{cell}}\varepsilon_c+\lambda\left\langle C_f\right\rangle^f}\right)-k_a\varepsilon_c,\end{aligned} \tag{8}$$

where the coefficients in (7) are defined as

$$\alpha = \frac{\varepsilon_c \lambda D^c_{\text{eff}} + (\varepsilon - \varepsilon_c) D^f_{\text{eff}}}{r},$$
$$\beta = \lambda D^c_{\text{eff}} - D^f_{\text{eff}}, \tag{9}$$
$$\delta = \varepsilon + (\lambda - 1)\varepsilon_c.$$

Equation (7) describes the changes of intrinsic glucose concentration of the fluid phase, $\langle C_f \rangle^f$, with respect to time and radius of the scaffold. Since a partition coefficient of 0.1 in (4) relates the intrinsic glucose concentration of the fluid phase to that of the solid phase, (7) explains the changes of glucose concentration in the cell colony phase too. Equation (9) describes the changes of the volumetric cell fraction with time and the radius of the cell-scaffold construct.

As it can be seen in (8), changes in cell volumetric fraction relies on the variation of the fluid phase glucose concentration which is described by (7). Therefore, (7) and (8) are coupled and must be solved simultaneously for simulating glucose transfer and cell growth in the cell-scaffold. The initial condition of the intrinsic glucose concentration of the fluid phase inside the cell-scaffold construct is defined as

$$\left\langle C_f \right\rangle^f (r, t = 0) = C_0, \tag{10}$$

where C_0 is glucose concentration of culture medium surrounding the scaffold. The initial conditions of volumetric cell fraction are defined for two initial cell-scaffold conditions where cells are seeded uniformly and nonuniformly as

$$\begin{aligned} &\text{(i)}\ \ \varepsilon_c (0 \le r \le R,\ t = 0) = \varepsilon_{c0} = 0.00548, \\ &\text{(ii)}\ \ \varepsilon_c (r = R,\ t = 0) = \varepsilon_{c0} = 0.00548; \\ &\qquad\ \ \varepsilon_c (0 \le r < R,\ t = 0) = 0, \end{aligned} \tag{11}$$

where $\varepsilon_c\,(0 < r < R,\ t = 0)$ and $\varepsilon_c\,(r = R,\ t = 0)$ are associated with uniform cell distribution throughout the scaffold and seeded cells on the scaffold surface, respectively. For boundary conditions of glucose concentration, fixed concentration and symmetry condition are considered for the surface and the center of the scaffold, respectively, as

$$\left.\frac{\partial \left\langle C_f \right\rangle^f}{\partial r}\right|_{r = 0, t} = 0,$$
$$\left\langle C_f \right\rangle^f (r = R, t) = C_0. \tag{12}$$

For volumetric cell fraction, symmetry condition at the scaffold center and no-flux condition at the scaffold surface are defined as

$$\left.\frac{\partial \varepsilon_c}{\partial r}\right|_{r = 0, t} = 0,$$
$$\left.\frac{\partial \varepsilon_c}{\partial r}\right|_{r = R, t} = 0. \tag{13}$$

2.3. Numerical Solution of the Model. The scaffold was divided into $N+1$ nodes where nodes of N and $N+1$ were the last node in the scaffold and the factious node in the culture medium surrounding the scaffold. Then, governing equations of (7) and (8) were discretized using implicit finite difference method. Applying boundary conditions, the discretization of (7) resulted in the following nodal equations for glucose transfer as

$$C^t_{f,i} = \frac{C^{t-1}_{f,i} + \left(4\Delta t \psi^t_i / 3\Delta r^2\right) C^t_{f,i+1}}{1 - \varphi^t_i \Delta t + \left(4\Delta t \psi^t_i / 3\Delta r^2\right) + \mu^t_i \Delta t} \quad (i = 1),$$
$$C^t_{f,i} = \frac{C^{t-1}_{f,i} + \left(\left(\alpha^t_i / \delta^t_i\right) + \left(\beta / \delta^t_i\right)\left(\left(\varepsilon^t_{c,i+1} - \varepsilon^t_{c,i-1}\right)/2\Delta r\right)\right)\left(\Delta t \left(C^t_{f,i+1} - C^t_{f,i-1}\right)/2\Delta r\right) + \left(\left(\Delta t \psi^t_i \left(C^t_{f,i+1} + C^t_{f,i-1}\right)\right)/\Delta r^2\right)}{1 - \varphi^t_i \Delta t + \left(2\Delta t \psi^t_i / \Delta r^2\right) + \mu^t_i \Delta t} \quad (1 < i < N), \tag{14}$$
$$C^t_{f,i} = \frac{C^{t-1}_{f,i} + \left(2\Delta t \alpha^t_i \left(C_0 - C^t_{f,i-1}\right)/3\Delta r \delta^t_i\right) + \left(4\Delta t \psi^t_i \left(2C_0 + C^t_{f,i-1}\right)/3\Delta r^2\right)}{1 - \varphi^t_i \Delta t + \left(4\Delta t \psi^t_i / \Delta r^2\right) + \mu^t_i \Delta t} \quad (i = N),$$

where the parameters of φ^t_i, μ^t_i, and ψ^t_i in (14) are defined as

$$\varphi^t_i = \frac{(1 - \lambda)\left(\varepsilon^t_{c,i} - \varepsilon^{t-1}_{c,i}\right)}{\Delta t \delta^t_i};$$
$$\mu^t_i = \frac{K \lambda \varepsilon^t_{c,i}}{\delta^t_i}; \qquad \psi^t_i = \frac{\beta \varepsilon^t_{c,i} + \gamma}{\delta^t_i}, \tag{15}$$

with α, β, and δ coefficients given in (9). Likewise, applying boundary conditions to (8) resulted in the discretized form of the equation as

$$\varepsilon^t_{c,i} = \frac{\varepsilon^{t-1}_{c,i} + \left(4\Delta t D_{\text{cell}} / 3\Delta r^2\right) \varepsilon^t_{c,i+1}}{1 - \theta^t_i \Delta t + \left(4\Delta t D_{\text{cell}} / 3\Delta r^2\right) + k_a \Delta t} \quad (i = 1),$$
$$\varepsilon^t_{c,i} = \frac{\varepsilon^{t-1}_{c,i} + \left(\Delta t D_{\text{cell}} / (2i - 1)\,\Delta r^2\right)\left(2i\varepsilon^t_{c,i+1} + (2i - 2)\,\varepsilon^t_{c,i-1}\right)}{1 - \theta^t_i \Delta t + \left(2\Delta t D_{\text{cell}} / \Delta r^2\right) + k_a \Delta t}$$
$$(1 < i < N),$$

Table 1: Properties and parameters for cellular, metabolic, cell growth kinetics and scaffold.

Property	Value	Reference
Cell density (ρ_c)	182 kgm^{-3}	Bush and Hall, 2001 [10]
Glucose effective diffusivity in cell colony (D^c_{eff})	1.0×10^{-10} m^{2}s^{-1}	Galban and Locke, 1999 [9]
Glucose effective diffusivity in the nutrient solution (D^f_{eff})	1.0×10^{-9} m^{2}s^{-1}	Galban and Locke, 1999 [9]
Glucose partition coefficient (λ)	0.1	Galban and Locke, 1999 [9]
Cellular maximum consumption rate (K)	0.03 s^{-1}	Galban and Locke, 1999 [9]
Initial porosity of the scaffold (ε)	0.92–0.96	Freed et al., 1994 [7]
Cell seeding efficiency (η_c)	0.60	Freed et al., 1994 [7]
Initial population of seeded cells (P_{c_0})	4×10^6 cells	Freed et al., 1994 [7]
Initial volumetric fraction of seeded cells (ε_c)	0.00548	Freed et al., 1994 [7]
Cell growth rate coefficient (k_g)	1.6×10^{-5} s^{-1}	Chung et al., 2006 [5]
Cell death rate coefficient (k_a)	3.3×10^{-7} s^{-1}	Chung et al., 2006 [5]
Contois saturation coefficient (k_c)	1.54	Galban and Locke, 1999 [9]
Random walk coefficient of cells (D_{cell})	1.7×10^{-14} m^{2}s^{-1}	Barocas et al., 1995 [11]

$$\varepsilon^t_{c,i} = \frac{\varepsilon^{t-1}_{c,i} + \left(4\Delta t D_{\text{cell}}/3\Delta r^2\right)\varepsilon^t_{c,i-1}}{1 - \theta^t_i \Delta t + \left(4\Delta t D_{\text{cell}}/3\Delta r^2\right) + k_a \Delta t} \quad (i = N), \tag{16}$$

where θ^t_i is defined as

$$\theta^t_i = \frac{k_g \lambda C^t_{f,i}}{k_c \rho_{\text{cell}} \varepsilon^{t-1}_{c,i} + \lambda C^t_{f,i}} \quad (1 \le i < N),$$
$$\theta^t_{i=N} = \frac{k_g \lambda C_0}{k_c \rho_{\text{cell}} \varepsilon^{t-1}_{c,i=N} + \lambda C_0} \quad (i = N). \tag{17}$$

Sensitivity analyses of glucose concentration and cell volumetric fraction were performed for different grid sizes (Δx) and time step sizes (Δt) at a fixed position of the scaffold. In addition to stability and accuracy of the solution, the speed of solution was taken into account for determination of time step size and grid size. The systems of equations of (14) and (16) were simultaneously numerically solved using Gauss-Seidel method.

2.4. Properties and Parameters. Table 1 presents properties associated with cartilage cells, the substrate, cell metabolism, and growth kinetics as well as initial scaffold porosity. The partition coefficient of 0.1 can describe glucose equilibrium condition between cell colonies and the nutrient solution in the scaffold. Values of the initial scaffold porosity and cell seeding efficiency are 92%–96% and 60%, respectively [7].

3. Results and Discussion

3.1. Determination of Mesh and Time Step Size. Figure 3 illustrates the contour plot of cell volumetric fraction (Figure 3(a)) and glucose concentration (Figure 3(b)) with respect to number of nodes and logarithm of time step size. As it can be seen in Figure 3(a), the number of nodes has no significant effect on cell volumetric fraction values at the scaffold radius of 1 mm for 5 days. However, the predicted value of cell volumetric fraction sharply changes when $\log(\Delta t)$ changes from 0 to −0.6 (where Δt is reduced from 1 to 0.1 day), and it eventually levels off at $\log(\Delta t)$ of −1.25 (Δt of 0.055 day). In the same way, Figure 3(b) illustrates the sensitivity of glucose concentration with respect to $\log(\Delta t)$ and number of nodes. As shown in the figure, the predicted values of glucose concentration have a significant sensitivity with respect to number of nodes when number of nodes increases from 5 to 34. The variation of predicted values of glucose concentration levels off at the number of nodes of 34. Also, for logarithmic values of time step size greater than −0.6 (Δt of 0.25 day), no significant sensitivity of predicted values of glucose concentration can be perceived. According to Figures 3(a) and 3(b), the time step size of 0.01 day and the number of nodes of 34 in which both cell volumetric fraction and glucose concentration have no sensitivity with respect to time step size and number of nodes were adopted for numerical simulation.

3.2. Time-Dependent Glucose Concentration Gradient across the Scaffold. Figure 4 illustrates simulation results for the variation of the intrinsic glucose concentration of the fluid phase in the cell-scaffold with time and the scaffold radius. As it can be seen, the initially uniform glucose concentration across the scaffold significantly drops within few hours after placing the scaffold in the culture medium due to the glucose cell consumption in the scaffold. However, due to the diffusional mass transfer resistance, the glucose concentration of the scaffold interiors is reduced faster than that of the scaffold locations close to the surface. The glucose concentration gradient across the scaffold increases with time until it reaches 2.7 kgm^{-3} after about 50 days for the interior locations of the scaffold.

3.3. Simulation of Cell Proliferation across the Scaffold. Figure 5 depicts the simulation results for the variation of cell volumetric fraction of the scaffold with time and the scaffold radius. Cell volumetric fraction increases with time for all scaffold locations; however, after about 20 days, the cell growth at the scaffold locations closer to the surface

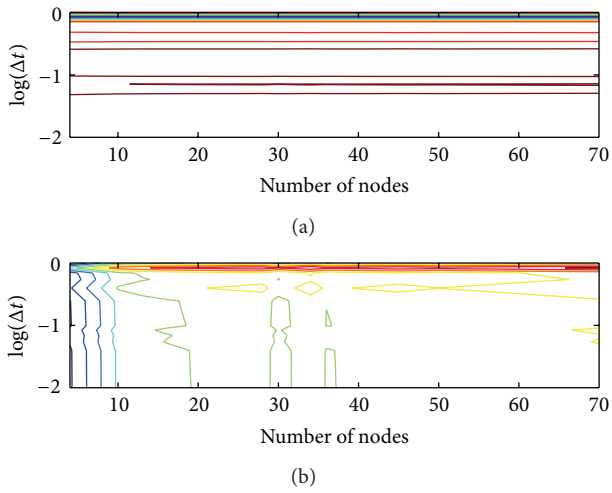

Figure 3: Sensitivity analysis of cell volumetric fraction (a) and glucose concentration (b) with respect to number of nodes and logarithm of time step size for a cell cultivation period of 5 days at the scaffold radius of 1 mm.

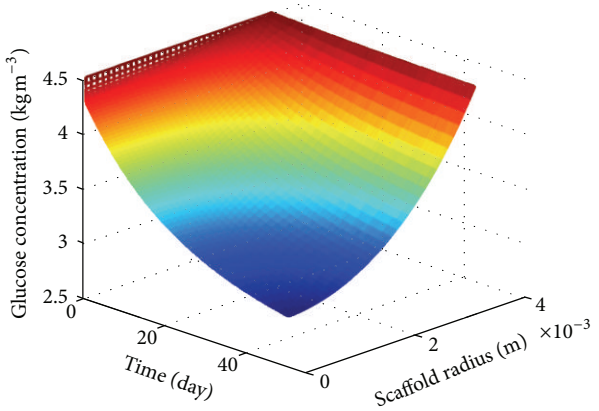

Figure 4: Simulation results for the fluid phase glucose concentration of the cell-scaffold with time and the scaffold position for an initial glucose concentration of 4.5 kgm^{-3}, initial cell volumetric fraction of 0.00548, and scaffold radius of 3.5 mm.

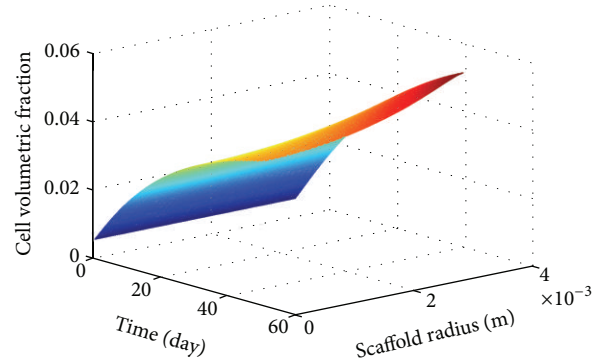

Figure 5: Simulation results for cell volumetric fraction of the cell-scaffold construct with time and the scaffold position for an initial glucose concentration of 4.5 kgm^{-3}, initial cell volumetric fraction of 0.00548, and scaffold radius of 3.5 mm.

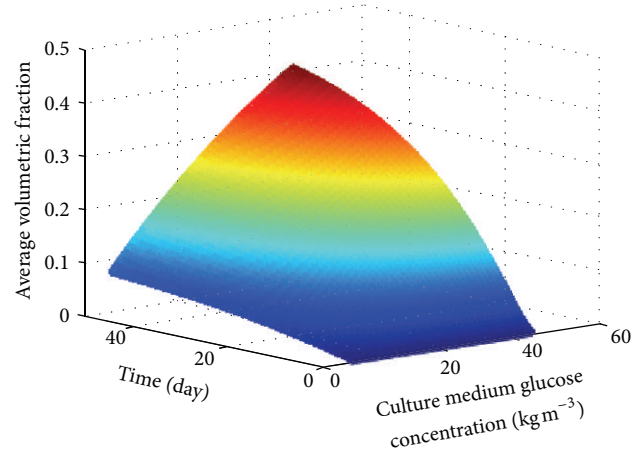

Figure 6: The effect of glucose concentration of the surrounding culture medium on the average cell volumetric fraction of the scaffold within 50 days.

becomes faster than that at the interior locations of the scaffold. It is associated with higher glucose concentration at the locations close to the surface rather than the locations close to the scaffold center. Mass transfer diffusion resistance causes lower glucose concentration in the center compared to the locations close to the scaffold surface. Lower glucose concentration of the interior locations decreases cell growth rate causing smaller cell volumetric fraction of the scaffold interior. As it can be seen, after 50 days, the cell volumetric fraction of the scaffold locations close to the surface is significantly higher than that of the scaffold interiors.

Figure 6 depicts the variation of the average volumetric cell fraction of the scaffold for different levels of glucose concentration of the surrounding culture medium within 50 days. Average cell volumetric cell fraction increases with time for all levels of culture glucose concentration; however, higher glucose concentration of the culture induces higher rate of increase in cell volumetric cell fraction. As shown in Figure 6, when the culture glucose concentration increases from 4.5 to 45 kgm^{-3}, the average cell volumetric fraction improves from less than 1% to 40% after 50 days.

Figure 7 illustrates the distribution of cell volumetric fraction across the scaffold within 50 days for initially uniform seeded cells (a) and seeded cells on the scaffold surface (b) at a culture glucose concentration of 4.5 kgm^{-3}. For initially uniform seeded cells (Figure 7(a)), a uniform cell growth distribution can be perceived within around 25 days. The gradient of cell population distribution within the scaffold increases with time after 25 days. It is because the higher volumetric cell fraction increases the scaffold tortuosity which reduces the effective diffusivity of glucose (D^f_{eff}). Smaller effective diffusivity of glucose (D^f_{eff}) of the scaffold results in higher mass transfer resistance for glucose to diffuse into the scaffold. Therefore, cells at the locations close to the scaffold surface can grow better than those located inside the scaffold, and it causes the gradient to increase

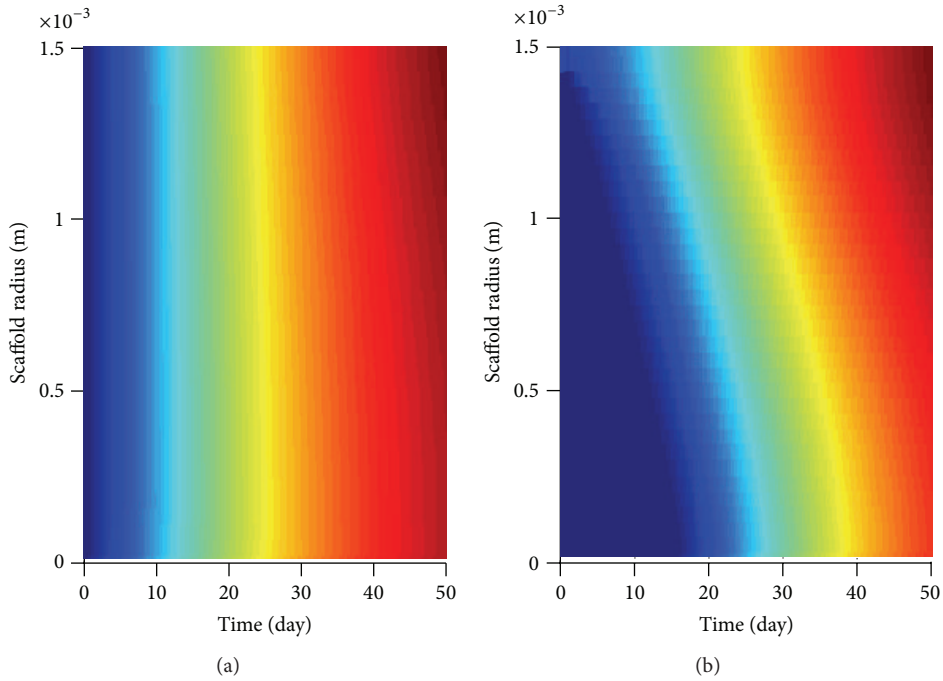

FIGURE 7: The effect of uniformly (a) and non-uniformly (b) initial cell distributions on the cell proliferation within the scaffold for a cell cultivation time of 50 days.

with time so that a cell population gradient has resulted after 50 days. Contrary to the initially uniform cell seeding pattern (biomanufacturing-based cell seeding), a significant cell population gradient can occur during the cell cultivation time when superficial cell seeding is applied (Figure 7(b)). As it can be seen in Figure 7(b), initially a sharp cell population gradient can be observed at the top of the scaffold due to the superficial cell seeding which provides a cell distribution on the scaffold surface but no cell distribution inside the scaffold. As the cultivation time passes, cells grow and migrate towards inside the scaffold such that cell population inside the scaffold will be no longer zero after 20 days. It indicates that after about 20 days, cells, which were initially seeded on the scaffold surface, have grown and migrated across the scaffold (Figure 7(b)). While the cell population keeps increasing across the scaffold, unlike the biomanufacturing-based cell seeding (Figure 7(a)), a cell population gradient (from higher cell population at the scaffold surface to the lower cell population at the scaffold bottom) exists for all cultivation times. Comparing Figures 7(a) and 7(b) indicates that a more uniform cell distribution with higher average cell volumetric fraction can be obtained after 50 days when cells are initially seeded across the scaffold by biomanufacturing-based cell seeding method.

4. Conclusion

Assessing the validity of LVA approach revealed that LVA method can be used for modeling glucose transfer and cell proliferation in the cell-scaffold construct. Simulation results indicated that diffusional mass transfer resistance plays an important role in glucose concentration gradient occurring across the scaffold within 50 days (Figure 4). When the glucose concentration in the medium is increased from 4.5 kgm^{-3} to 45 kgm^{-3}, cell volumetric fraction increases from 6% to 40% after 50 days (Figures 5 and 6). In addition, assuming that the initial cell distribution during the cell seeding is uniform, simulation results indicate that more uniform cell distribution with higher average cell volumetric fraction within the scaffold can be resulted. Due to the small size of the scaffold, it seems that the assumption of only radial dimensional mass transfer is inappropriate. For future works, the simulation can be significantly improved if the two-dimensional governing equations of (5) and (6) are used for simulation instead of (7) and (8). The model can be used for simulation of cell proliferation of other types of cells (i.e., Schwann cell) and for prediction of an appropriate time of cell cultivation before implantation. Also, in order to identify the uncertainty of the uniformity of cell distribution for the biomanufacturing cell seeding, a statistical function describing the degree of uniformity of cell distribution across the scaffold will need to be identified and included in the model.

References

[1] L. G. Griffith and G. Naughton, "Tissue engineering—current challenges and expanding opportunities," *Science*, vol. 295, no. 5557, pp. 1009–1014, 2002.

[2] D. W. Hutmacher, "Scaffolds in tissue engineering bone and cartilage," *Biomaterials*, vol. 21, no. 24, pp. 2529–2543, 2000.

[3] R. Langer and J. P. Vacanti, "Tissue engineering," *Science*, vol. 260, no. 5110, pp. 920–926, 1993.

[4] J. O. Hollinger and A. Chaudhari, "Bone regeneration materials for the mandibular and craniofacial complex," *Cells and Materials*, vol. 2, pp. 143–151, 1992.

[5] C. A. Chung, C. W. Yang, and C. W. Chen, "Analysis of cell growth and diffusion in a scaffold for cartilage tissue engineering," *Biotechnology and Bioengineering*, vol. 94, no. 6, pp. 1138–1146, 2006.

[6] D. Pazzano, K. A. Mercier, J. M. Moran et al., "Comparison of chondrogensis in static and perfused bioreactor culture," *Biotechnology Progress*, vol. 16, no. 5, pp. 893–896, 2000.

[7] L. E. Freed, G. Vunjak-Novakovic, J. C. Marquis, and R. Langer, "Kinetics of chondrocyte growth in cell-polymer implants," *Biotechnology and Bioengineering*, vol. 43, no. 7, pp. 697–604, 1994.

[8] M. C. Lewis, B. D. MacArthur, J. Malda, G. Pettet, and C. P. Please, "Heterogeneous proliferation within engineered cartilaginous tissue: the role of oxygen tension," *Biotechnology and Bioengineering*, vol. 91, no. 5, pp. 607–615, 2005.

[9] C. J. Galban and B. R. Locke, "Analysis of cell growth kinetics and substrate diffusion in a polymer scaffold," *Biotechnology and Bioengineering*, vol. 65, pp. 121–132, 1999.

[10] P. G. Bush and A. C. Hall, "Regulatory volume decrease (RVD) by isolated and *in situ* bovine articular chondrocytes," *Journal of Cellular Physiology*, vol. 187, no. 3, pp. 304–314, 2001.

[11] V. H. Barocas, A. G. Moon, and R. T. Tranquillo, "The fibroblast-populated collagen microsphere assay of cell traction force, part 2: measurement of the cell traction parameter," *Journal of Biomechanical Engineering*, vol. 117, no. 2, pp. 161–170, 1995.

[12] M. Kaviany, *Principles of Heat Transfer in Porous Media*, Springer, New York, NY, USA, 2nd edition, 1995.

[13] D. W. Hamilton, M. O. Riehle, W. Monaghan, and A. S. G. Curtis, "Articular chondrocyte passage number: influence on adhesion, migration, cytoskeletal organisation and phenotype in response to nano- and micro-metric topography," *Cell Biology International*, vol. 29, no. 6, pp. 408–421, 2005.